

Passive Diffusion Processes Govern the Initial Stages of Cell Penetration into Electrospun Scaffolds



Casey PG¹ and David G Simpson^{2*}

¹Department of Biomedical Engineering, USA

²Department of Anatomy and Neurobiology, Virginia Commonwealth University, USA

Submission: April 13, 2017; Published: May 23, 2017

*Corresponding author: David G Simpson, Department of Anatomy and Neurobiology, Virginia Commonwealth University, USA,
Email: David.Simpson@VCUhealth.org

Abstract

We explore how the passive the diffusion of cells and active migration events interact with scaffold structure to modulate the extent to which electro spun PCL scaffolds are infiltrated by dermal fibroblasts in tissue culture. The data indicate that passive processes predominate during the first 24hr of culture. Infiltration was observed to a nearly equal extent in scaffolds produced by air impedance electro spinning in the presence and absence of air flow through the mandrel pores, demonstrating that electrostatic edge effects play a substantial role in producing the regional changes in fiber density that typify this fabrication technique. We conclude that cells preferentially sieve across the Z axis through these macro pores; however, a similar mechanism appears to be at work in scaffolds produced by conventional electro spinning techniques. The passive sieving hypothesis is supported by two lines of experimental evidence. First, a sub-population of cells rapidly populate the deeper recesses of the electro spun scaffolds over the first 24hr of culture, subsequent penetration is nearly non-existent. Second, even cells killed by Para formaldehyde incubation are observed to penetrate up to 300um deep into these scaffolds. Cyclic exposure to trypsin at 24hr intervals dramatically increased the number of cells that infiltrated electro spun scaffolds.

Introduction

The inability to rapidly seed and populate electro spun tissue engineering scaffolds at high cell density in tissue culture represents a long recognized limitation to this emergent technology. This, despite the interconnected nature of pores that are present in these scaffolds. A broad spectrum of electro spun scaffolds composed of natural [1] synthetic polymers [2,3] and blends of natural and synthetic polymers [4] are extensively infiltrated by inflammatory, interstitial and vasculogenic cells when they are implanted in situ [5]. Cell infiltration is likely far more efficient in this setting due to a variety of variables including the presence of an intact immune response and the penetration of soluble of grow factors from the surrounding environment. The environmental factors that lead to the penetration of cells into implanted electro spun scaffolds have not been fully defined or even remotely reproduced in tissue culture. A fundamental objective of the classical tissue engineering paradigm is to produce tissues in vitro that can ultimately be used to replace or augment the function of damaged, diseased or otherwise missing organs. To fulfill this promise, regardless of the identity of the

scaffold, strategies to fully populate tissue engineering scaffolds in vitro must be developed.

Experiments in tissue culture environments that are nominally 3D in nature demonstrate that scaffold and fiber stiffness, fiber density, cell-matrix adhesion properties and proteolytic events all serve to modulate the rate at which cells can migrate [5-8]. In typical experiments, velocity is measured in cells moving in the X-Y orientation on tissue culture plastic coated with fibers of varying density and or physical properties. While revealing, this approach fails to capture the behavior of cells in the unique 3D environment of an electro spun matrix and it might be more accurate to state these experiments define the variables that govern migration rates on a 2D surface exhibiting complex topographical features (i.e. the fiber bundles) rather than a 3D environment. On such a surface there is virtually no depth in the Z direction where pore size and geometry will represent a major impediment to motility [9]. In a truly 3D environment cells are surrounded on all sides by the constituent elements of the surrounding matrix, regardless of its composition. This consideration is critically important in

a 3D electro spun scaffold that lacks guidance cues to promote the migration in the Z direction [10] the fibers of these scaffolds are largely arrayed into layers that lie parallel with the dorsal surface of the construct.

Under base line conditions the prototypical tissue culture environment appears to lack the appropriate cues necessary to drive cells to penetrate into the deeper regions of a 3D electro spun matrix. Cells seeded onto the external surfaces of these structures clearly migrate and proliferate much like they do on a fiber-coated, nominally 3D surface. However, penetration is largely limited to a few cell diameters in depth on almost all types of electro spun surfaces composed of physiologically sized fibers. Once the cells have entered the scaffold they appear to reach a thermodynamic equilibrium and without further impetus fail to penetrate into the deeper regions of the scaffold.

In the present study we explore the processes that govern cell penetration into conventional electro spun scaffolds and those produced by air impedance electro spinning [11]. Air impedance electro spinning uses a hollow mandrel engineered with a series of pores as a collecting target. Air is introduced at various velocities into the center of the mandrel and then flows out of the pores. The air flow is designed to inhibit the deposition of fibers in the vicinity of the pores and thereby reduce the local density of the scaffold in a regional fashion in order to facilitate cell penetration.

Materials and Methods

Electro spinning

All reagents Sigma unless noted. Polycaprolactone (PCL: 65,000 M.W.) was dissolved in trifluoroethanol (TFE; 150 or 250mg/mL) and placed into a syringe. Syringes were capped with an 18-gauge blunt-tip needle and placed into a syringe driver (Fisher Scientific) programmed to deliver a total volume of 3mL of solution at a constant rate of 9mL/hr. Spell men, low current, high voltage power supplies were used to generate electric fields (17-19kV) across a 20cm air gap. A rotating (700rpm) and translating (4cm/s over a 12cm distance) mandrel (6mm diameter) was used as a target. After electro spinning was complete scaffolds were cut longitudinally from the mandrel and stored in a desiccators until needed.

Air impedance electro spinning

Conditions used to electro spun conventional scaffolds were replicated with the exception that a hollow perforated stainless steel mandrel equipped for air impedance was used as a target to collect the scaffolds [11]. The collection mandrel (6mm in diameter) was engineered with 0.75mm diameter circular perforations spaced every 2.0mm circumferentially (center-to-center) around the mandrel and every 1.5mm down the long axis (center-to-center) of the mandrel. Air flow was introduced into the mandrel at pressures of 0kPa (static), 100kPa, and 300kPa.

Computational fluid dynamics (CFD)

All computer drawings and meshes were generated using Gambit (Version 2.4). Fluid model simulations were performed in Fluent (Version 12.0) using 1,000 iterations or until convergence was achieved. Graphical representation of the fluid models was visualized using Tec plot [10].

Cell culture

Human dermal fibroblasts (hDF, Cascade Biologics C-013-5C) were cultured in DMEM-F12 (Gibco) plus 10% fetal bovine serum (FBS, Hyclone) and 1% penicillin/streptomycin (P/S, Invitrogen). Electro spun scaffolds punch cut into 6mm diameter circles were sanitized in 70% ethanol for 30min, rinsed 2X in phosphate buffer saline (PBS) and transferred to serum free media. For cell seeding (25,000 cells) a sterile glass cloning ring was placed onto the scaffolds. Cloning rings were removed after 24hr; cells were cultured at 37°C and 5% CO₂. Media changed every 3 days.

To explore how passive processes govern cell penetration into electro spun scaffolds cells were suspended in PBS supplemented with 5% para formaldehyde for 30 minutes. The dead cells were rinsed in PBS supplemented with BSA to block any reactive groups prior to plating onto electro spun scaffolds.

Cultures plated into electro spun scaffolds also were exposed to daily 15 minute incubations in trypsin (0.025%) prepared in PBS daily beginning on day 1 after plating for 5 days and isolated for analysis on day 7. Control cultures were exposed to a 15 incubation in PBS+EDTA in the absence of trypsin. After each incubation cultures were rinsed and returned to media.

Cryo sectioning

Scaffolds were fixed 10min in 10% glutaraldehyde, rinsed in PBS and transferred to 30% sucrose solution in PBS for three days at 4°C. Samples were infiltrated with Optical Temperature Cutting compound (OTC), frozen and cut en face into 50µm thick sections. Cut samples were placed immediately in to PBS and stored at 4°C. Cell nuclei were stained with 4',6-diamidino-2-phenylindole (DAPI). This approach provides a more comprehensive analysis of cell distribution than conventional cross sectional analysis (sections taken perpendicular to the surface of the scaffold) and allows us to reconstruct the distribution of cells in 3D [12].

Image analysis and 3D reconstruction

All images were captured on a Nikon TE300 microscope using a 10x or 20x objective using a DXM 1200 digital camera, images were collected at a resolution of 1280x1024. A bright field image was captured in conjunction with each corresponding fluorescence image of the DAPI stained nuclei. Bright field images were overlaid with corresponding fluorescence images in Adobe and combined using the photo merge function. Individual optical images from each frozen face section were assembled

using fiduciary marks captured in the bright field image into a montage of the entire 6mm diameter, 50um thick frozen sections. This process was repeated for each 50um thick section containing cells, once the entire depth of the scaffold was imaged and reconstructed as a montage the bright field images of the scaffold were removed using a threshold filter. Montage images were imported into Google Sketch Up for 3D reconstruction. DAPI stained nuclei were counted and then converted into cylinders for visualization in the 3D reconstruction. Full details see Grey and [12].

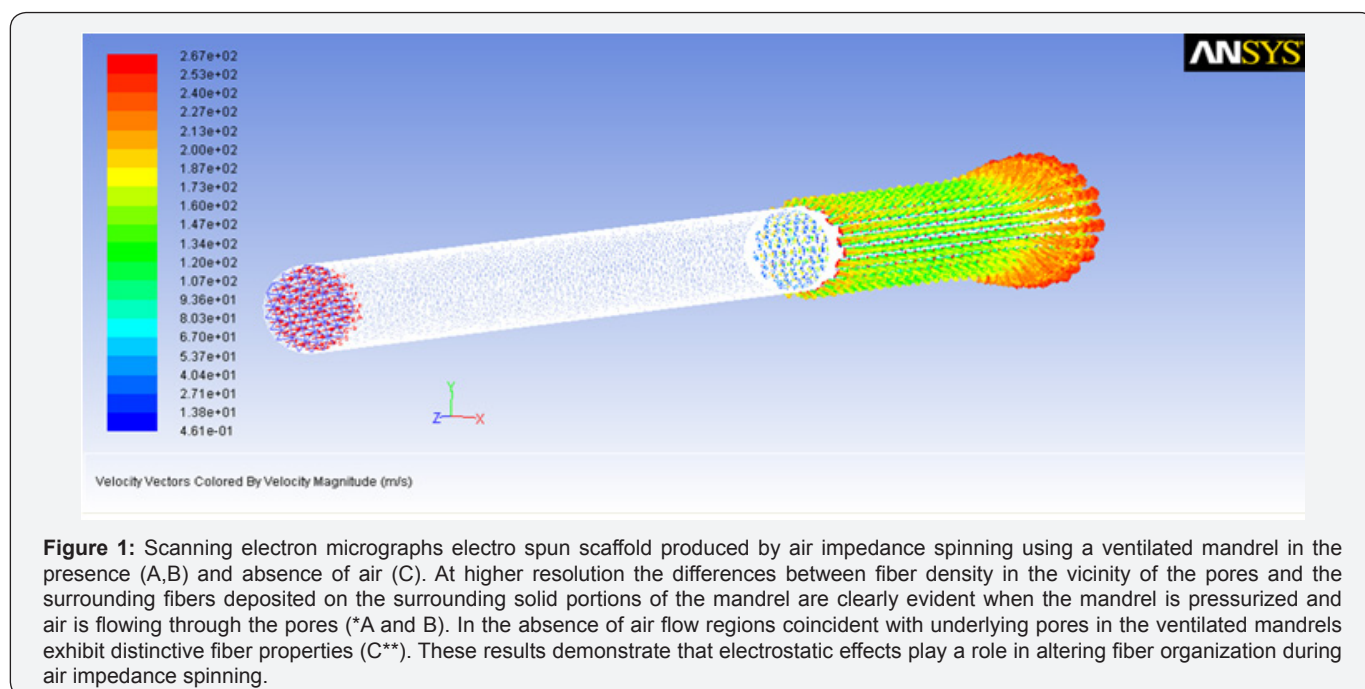
Statistics

All data sets were analyzed in Sigma Plot and screened using ANOVA. The Holm-Sidak method was used for pair wise comparisons. P values as provided. Graphical depictions represent ± the standard error unless otherwise noted.

Results

Air impedance electro spinning

Computational Fluid Dynamics Air impedance electro spinning was designed to produce scaffolds exhibiting systematically placed macro-pores by forcing air through openings engineered into the target mandrel. Fiber deposition is altered in the vicinity of the openings in the mandrel, presumably by the outflow of air through the mandrel ports. This results in the formation of macro pores that are designed to facilitate cell penetration by providing regional domains of decreased fiber density. We note, in the absence of air flow regional variations in fiber density are still observed in conjunction with the underlying ports of the mandrel, suggesting that air flow and electrostatic edge effects combine to alter fiber deposition in these domains (Figure 1).



Computational Fluid Dynamics (CFD) was used to explore the assumptions that underlie air impedance electro spinning. Theoretically, it is necessary to produce an even outward flow of air through the pores of a ventilated mandrel in order to produce periodic macro pores that exhibit similar structural properties. CFD modeling experiments demonstrate this condition is difficult to achieve, and given the apparent electrostatic edge effects associated with the engineered mandrel ports, may not be necessary. At an inlet pressure of 100k Pa CFD predicts that flow is very heterogeneous along the length of our model ventilated mandrel.

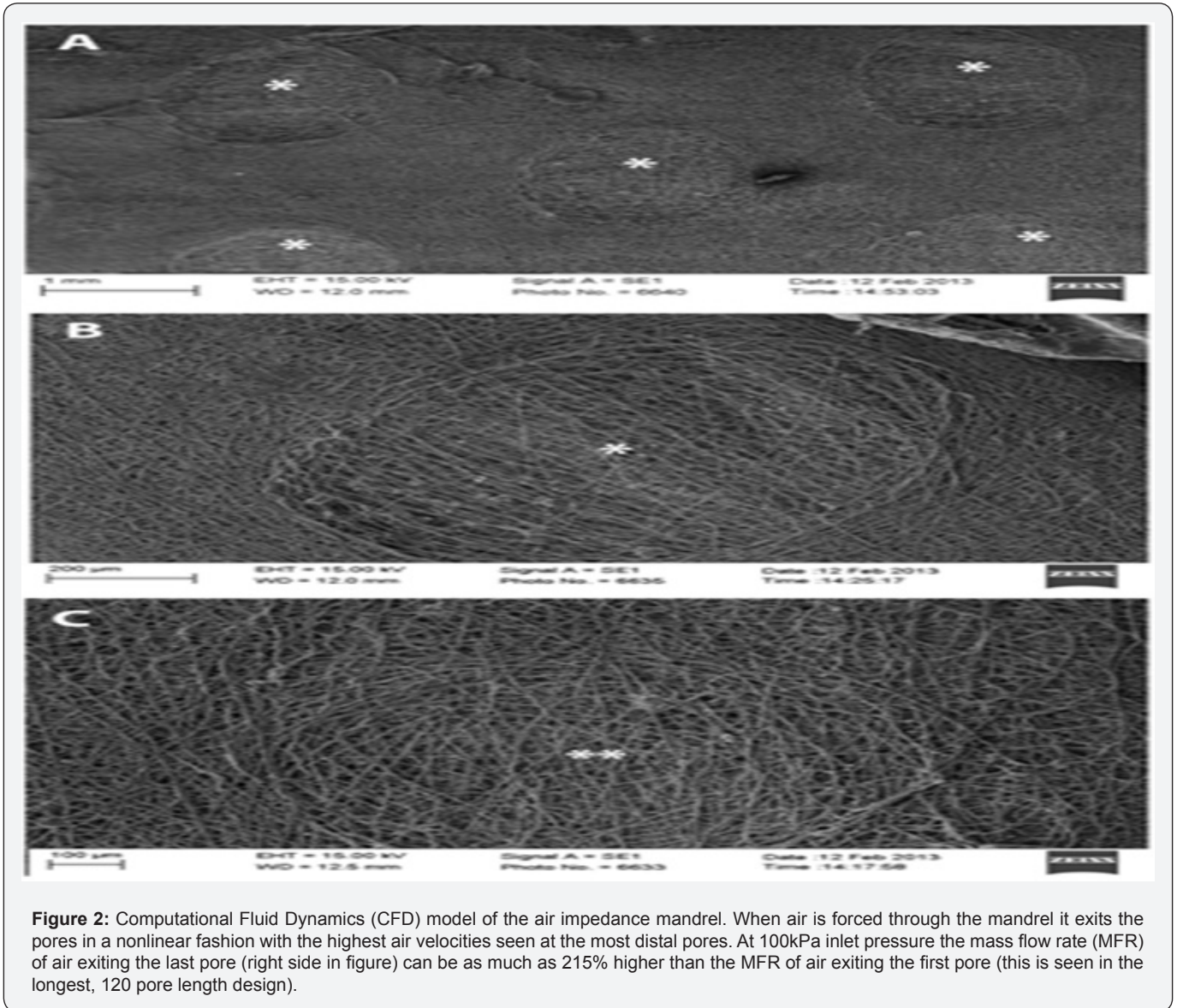
Figure 2 offers a convenient visualization of air velocity with respect to pore location in a ventilated mandrel. In this example the mandrel exhibits 120 pores spaced apart at 1.5mm internals (pore center to center) along its length, air is introduced at the

proximal end of the mandrel and the distal end of the mandrel is sealed. Both the color and length of the vectors presented in this figure are correlated to velocity (e.g. highest exit velocities are depicted in “long” red bars). Especially notable is the prominent distal velocity bulge that represents increased air velocities predicted at the pore regions at the end of the mandrel farthest away from the inlet air source. The bulk of the air travels down the length of the mandrel and preferentially exits pores located at the distal end of the mandrel. In practical use this disparity of flow is readily detectable by touch when such a mandrel is in use.

The introduction of various internal geometries into the mandrel proved largely unsuccessful at altering the preferentially exit of air from the distal pores. The most effective modification to the mandrel design was simply reducing the total length of the mandrel. Through this approach we were able to reduce the mass

flow rate (MFR in (kg/s) differential (most proximal pore vs. most distal pore) from 215% in the 120 pore model down to 99% by reducing the “pore length” of the mandrel to 60 pores and finally down to 20% by reducing the “pore length” to 30 pores (while maintaining the same pore spacing-data not shown). While these results show that differences in air flow across the length of the mandrel can be reduced, there were no obvious simple design

modifications that could be implemented to even out the flow through the pores. To account for these properties we chose to use only electro spun material deposited onto the proximal pore regions of a mandrel exhibiting a 120 pore length. While these regions displayed the least amount of air flow in our CFD models the pores in these domains exhibited the most uniform flow.



To justify this approach, we compared the MFR (kg/s) of the air flowing through each pore down the length of the mandrel. Based on repeated CFD (N=3) runs we determined that the most proximal 75% of the scaffold (pores 1-41) exhibited air flow rates that were not significantly different from one another and therefore should produce a scaffold exhibiting consistent physical properties (Figure 3). By comparison, the remaining

distal pores (pores 42-52) exhibited significantly higher air flow rates and do not represent a consistent fabrication environment (Figure 4). The MFR in the distal pores varied so abruptly (pore 52 displayed significantly higher flow rates compared to pores as close as pore 48, p=. 009) that any test samples taken directly adjacent to each in this region other would have been fabricated under very different conditions.

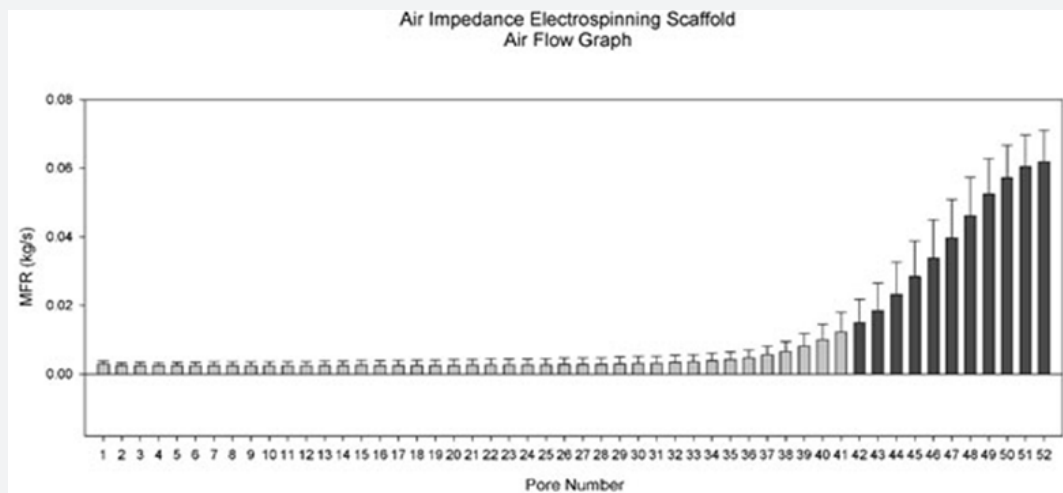


Figure 3: Mass flow rates (kg/s) were obtained from pores down the length of the air impedance mandrel model. Pore 1 represents the pore closest to the air source (most proximal pore, on the valve side) and pore 52 represents the pore most distal to the inlet air source. Using pore 1 as a control, mass flow rates from pore 42 through 52 (the last pore) were found to be significantly higher (see dark grey) than mass flow rates in each of pores 1-41 (light grey). P-values for pores 43 through 52 were <0.001 while pore 42 exhibited a p-value of 0.021.

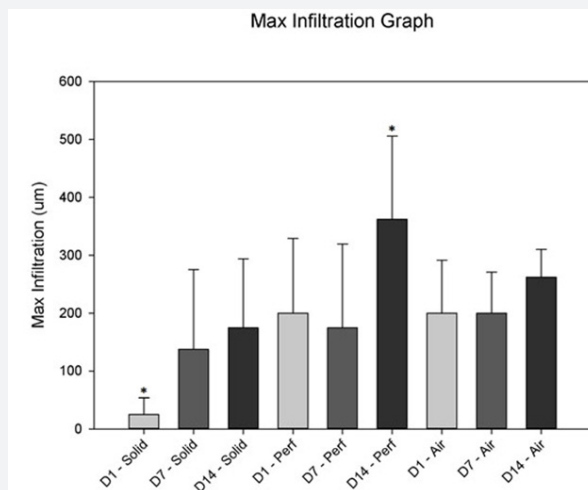


Figure 4: Comparison of maximum cellular infiltration on different scaffold types and throughout the three different time points. No significant differences were found across the treatment groups. Where solid=scaffolds collected on a conventional solid mandrel, Perf=scaffolds collected on a perforated mandrel in the absence of air flow and Air=scaffolds collected on the proximal regions of a perforated mandrel subjected to an inlet pressure of 100 kPa (where air flow is predicted to be relatively uniform as judged by CFD).

Cell culture experiments

We cultured human dermal fibroblasts (HDF) for varying intervals of time on scaffolds produced using a solid mandrel (“conventional electro spinning”), a perforated mandrel subjected to an inlet pressure of 100kPa and a perforated mandrel with no air flow. For constructs produced on the ventilated mandrels we only collected scaffolds that were recovered and prepared for cell culture from the proximal regions of the mandrel where CFD predicted air flow to be the most uniform. We made no effort to set a minimal threshold number of cells to count inside the scaffolds; rather we plated an equal number of cells on each scaffold and determined the maximal depth reached on each scaffold. Plotting

the maximum cellular infiltration depths vs electro spinning conditions as a function of time revealed very little difference across the treatment groups (Figure 5). Surprisingly, scaffolds collected onto a perforated mandrel in the absence of air flow appeared to support cell infiltration to approximately the same degree as those scaffolds collected with air flow.

After day one of culture, cells plated onto a conventional scaffold were limited to the first 50um of the scaffold. In contrast cells were found as deep as 200um in the scaffolds prepared on the perforated mandrels in the presence and absence of air flow (Figure 5). It is clear from these results that electrostatic edge effects associated with perforations in the electro spinning

mandrel likely disturb the fiber deposition nearly as much as the flow of air. Cells penetrated to an equal degree during the initial states of culture in scaffolds fabricated with and without

air flow. After the initial 24hr incubation there was virtually no further penetration into the scaffolds prepared on the perforated mandrels over the next 14 days.

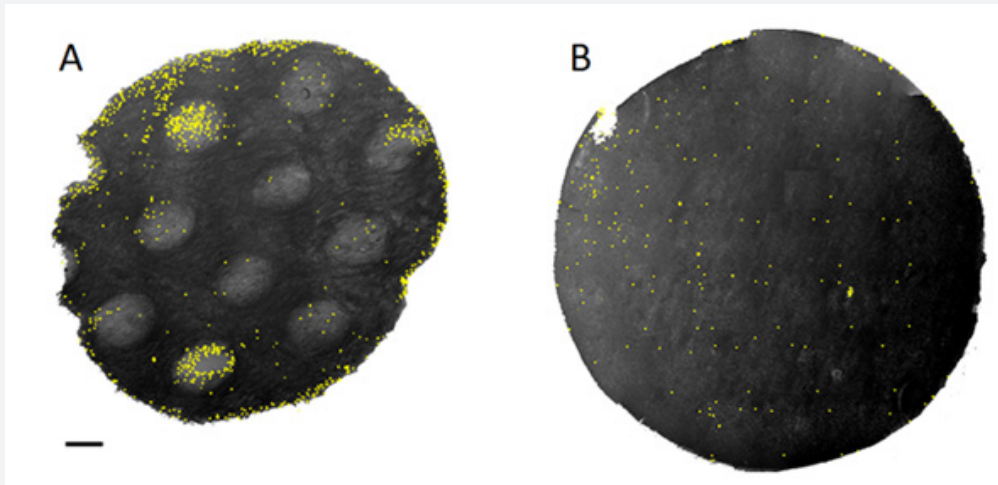


Figure 5: (A and B) 150mg/mL PCL electrospun scaffold fabricated on a perforated mandrel with no air flow (0kPa) and (B) 150mg/mL PCL electrospun scaffold fabricated on a solid mandrel. Sections taken at a depth of 50 μ m, cell nuclei shown in yellow. Both scaffolds display scattered cells, however, cells appear at a higher density in association with the macro-pore regions of scaffolds collected on a ventilated mandrel (A). We note the 150mg/ml PCL solution was used in these experiments to reduce the size/volume of the inter fiber spaces to emphasize the role of macropores in the promotion of cell penetration.

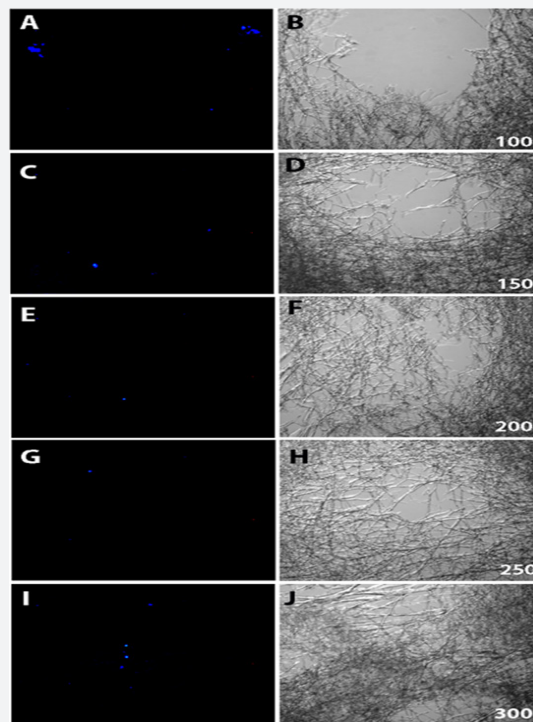


Figure 6: Sieving of Para formaldehyde fixed cells into a scaffold. Serial frozen sections through a scaffold fabricated on a perforated mandrel in the absence of air flow. Sections were taken through the depth of a single macro pore with the first section representing a depth of 100 μ m into the scaffold, subsequent sections taken at 50 μ m intervals. Panels A, C, E, G and I depict DAPI staining of nuclei. Note the detection of nuclei throughout the depth of the macro pore. Panels B, D, F, H and J depict corresponding bright field images. Electrostatic effects on scaffold structure are clearly evident to considerable depth, note how fiber density gradually increases as a function of depth in the scaffold macro pore.

To penetrate a scaffold by active migration events to a depth of 200 μ m over a 24hr interval would require a polarized and sustained migration velocity along a straight trajectory of approximately 8 μ m per hour (200 μ m of depth/24hrs), this despite the tortuous nature of the interconnected pores of an electro spun matrix. This velocity is possible and well within the capacity of many types of interstitial cells in vitro on a 2D surface [13], however it seems untenable that cells would sustain migration at such a velocity along a linear polarized tract in the environment afforded by an electro spun matrix.

Critically, two questions must be asked of these results. First, if cells can reach a depth of 200 μ m over the first 24hr by an active migration process why the deeper regions of the scaffolds are so sparsely populated after 7 days? and, secondly, why should cells on the dorsal plating surface cease further movement after 24hr and not continue to penetrate into the scaffold as a function of time in culture? Our results suggest that variables beyond active migration govern cell penetration in these scaffolds. It is clear that the macro pores must play a role in the process; perceived cell density is highest in regions immediately subjacent to these regions (Figure 4). To investigate the role of passive processes in the penetration of cells into air impedance scaffolds we incubated cells in par formaldehyde and then plated the dead cells for 24hr. At the conclusion of the "plating" interval dead cells were found to be present as deep as 300 μ m into the scaffolds (Figure 6).

These data demonstrates that cells passively sieve into the spaces afforded by an electro spun matrix and become lodged within the pore spaces when the volume of those spaces limits further penetration. In conventional tissue culture live cells will attach to a variety of surfaces through non-specific electrostatic interactions, spread out and begin to express elements of the extracellular matrix. These events must largely be reproduced within the 3D environment of an electro spun matrix and likely greatly suppress cell penetration [14]. If cells that have established early contacts with the fibers of the matrix could be systematically dislodged from those surfaces penetration into deeper regions of the scaffold might be achieved. To explore this hypothesis we examined how repeated exposure to trypsin might disrupt early cell matrix interactions and promote cell penetration into electro spun constructs.

Trypsin digest is the classical method used to disrupt cell matrix adhesions in tissue culture. To explore the utility of this method with cells trapped within an electro spun matrix we plated cells onto electro spun scaffolds and exposed them to daily 15min incubation in trypsin. In these experiments we utilized conventional scaffolds electrospun onto a solid mandrel using 250mg/ml PCL solutions. It is clear from cell counting data, (Figure 7 & 8), cross sectional analysis and 3D reconstructions (Figure 9) that cyclic trypsin treatments can promote increased cell penetration into electro spun scaffolds.

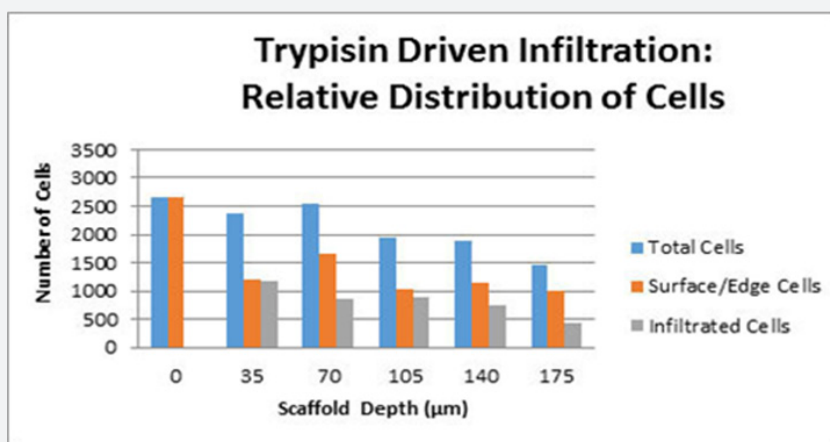


Figure 7: Cell penetration in the presence and absence of cyclic trypsin incubations after 7 days in scaffolds prepared on a solid mandrel using 250mg/ml PCL solutions. Cell counting data as a function of scaffold depth taken at 50 μ m intervals from frozen sections stained with DAPI. There is a dramatic increase in the number of cells that penetrate into the deeper recesses of a scaffold in response to cyclic incubations in trypsin. Cell counting data was subdivided into three specific categories where Total cells=Surface & edge + infiltrated. Surface cells are those cells that remain on the dorsal surface of the scaffold and edge cells represent those cells within 100 μ m of the lateral edges of the scaffolds. Infiltrated cells are those cells deep to the first 50 μ m thick frozen section (plating surface) farther within the confines of the 3D space defined by the electrospun scaffold. This approach was done to eliminate the contributions of cells that may have spilled over the edges of the scaffolds and then penetrated into the fiber layers from the lateral borders into the constructs (Grey and Simpson 2015).

Discussion

These data indicate that passive processes largely govern the penetration of cells into an electro spun scaffold composed of a synthetic polymer. Cells sieve into the interconnected pores across the Z axis over the first 24hr. This conclusion is supported

by two lines of experimental evidence. First, a sub-population of cells rapidly populate the deeper recesses of an electro spun scaffold over the first 24hr of culture, subsequent penetration is nearly non-existent and a large population of cells remains on the dorsal plating surfaces of the scaffolds. Second, even

par formaldehyde treated cells are observed to penetrate into the scaffolds. The lack of physical guidance cues likely limits the contributions of active migration in the penetration of cells

across the Z axis of these constructs. The active events of cell migration, when they take place, appear to predominately occur in parallel with the fiber layers rather than across the fiber layers.

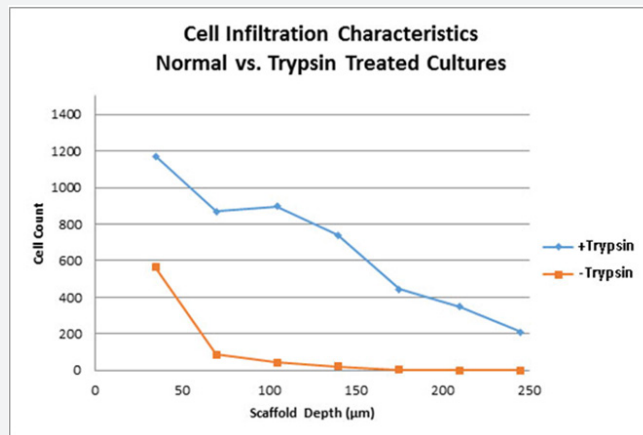


Figure 8: Summary of cell counting data presented in Figure 7. The exponential decay of cell count vs. scaffold depth is typical of control scaffolds treated at 24 hr intervals with a 15min PBS incubation. Scaffolds treated with trypsin exhibit far more cells at each depth assayed, cell counts in these cultures exhibit a nearly linear trend line ($r^2 = 0.9483$) as a function of scaffold depth.

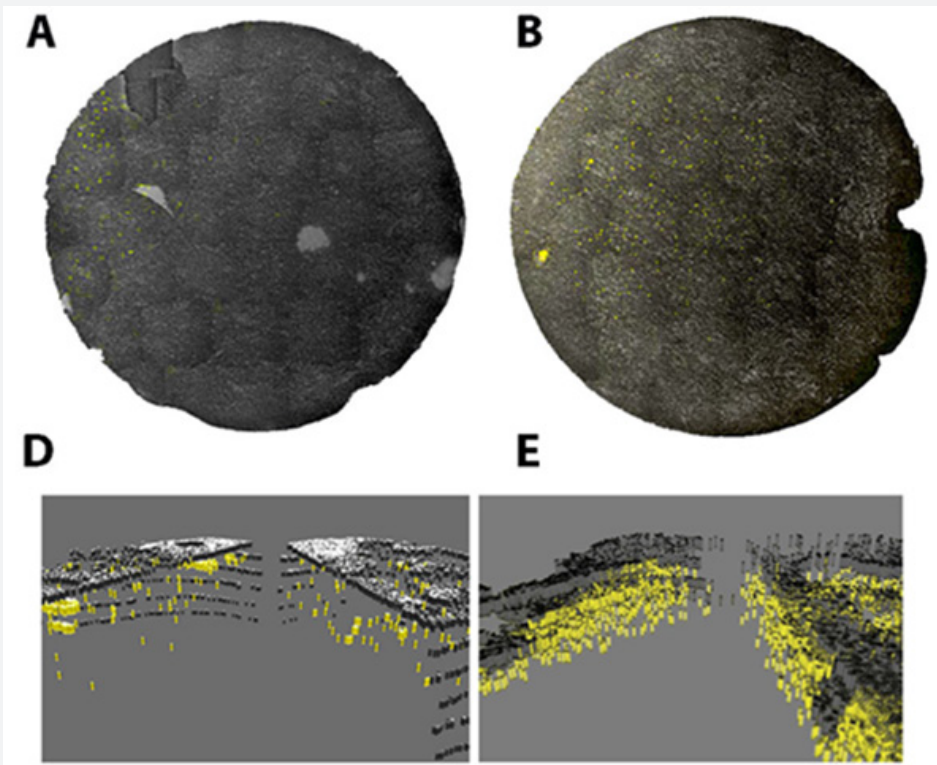


Figure 9: Cells cultured for 7 days plus or minus trypsin. DAPI staining reveals that control scaffolds (no trypsin) exhibit a low density, scattered population of cells at a depth of 150µm (A). In contrast, scaffolds treated with trypsin at daily intervals exhibit far more cells at this depth (B). The differences are clearly evident in the 3D reconstructions of these representative scaffolds (D and E). Scaffolds were frozen, cut into 50 µm thick sections and stained with DAPI. In the 3D reconstruction experiments the images were processed through a threshold filter to remove scaffold fibers, leaving the DAPI stained nuclei. Nuclei located within the scaffold are depicted as yellow cylinders, nuclei located on the surface or sides of the scaffold depicted as gray cylinders. The increased cell density throughout the scaffold treated with trypsin is clearly evident. These images represent a tangential view of the cylindrical scaffolds in which the scaffolds have been digitally cut in half along the central axis and then spread open to reveal details of the cell distribution within the deeper regions of the scaffolds.

Air impedance electro spinning was developed to promote the infiltration of cells across the Z axis of an electro spun scaffold [11]. The introduction of systematically placed regions of lower fiber density produced by air flow through a ventilated mandrel is intended to increase the porosity of a scaffold without substantially compromising its material properties. Our data (Figure 5) demonstrate that electrostatic edge effects play a central role in producing macro pores in these scaffolds. Given these results it would appear that very little advantage is to be gained by impressing air flow into this system, CFD modeling reveals that achieving an equal air flow-even in the absence of fiber deposition- is difficult to achieve, even on a small scale. However, we recognize that air effects may have more pronounced effects on modulating fiber density on thicker constructs.

The decreased fiber density associated with the macro pores fosters increased cell penetration (Figure 4), albeit this penetration appears to be primarily by passive sieving of cells into the scaffolds. We note that scaffolds fabricated with native proteins may be less likely to support sieving as well as a purely synthetic scaffold. The cell specific adhesion sites of such matrix would provide far more stable cell-matrix contacts than the non-specific electrostatic interactions that govern the early stages of contact between a cell and a synthetic biomaterial.

Constituents of the native extracellular matrix are arrayed in a many different orientations (X,Y and Z), in contrast, the fibers of an electro spun scaffold are deposited as a series of discreet layers in which the longitudinal axis of the fibers lies parallel to the target mandrel. This structural characteristic provides very large pore spaces between the fiber layers along the X-Y axis, a characteristic that provides very little impediment to movement along this axis (parallel to the dorsal surface). Previous experiments from our laboratory suggest that cells deep in a scaffold along the periphery of the construct largely originate with cells that spill over the edge of the construct during cell plating and have entered the scaffold along its lateral borders [12]. We have explored this consideration by producing cylindrical electro spun nerve guides composed of linear, parallel arrays of fibers [15]. The “enhanced porosity” or perhaps the lack of physical barriers present between the longitudinally arrayed fibers in combination with the guidance cues provided by the polarized fiber tracks in these devices provide a potent mix of signals to promote directed cell migration and axon elongation in vitro and in vivo [10,16].

The pores spaces present in an electro spun scaffold along the Z direction, while extensively interconnected, are far smaller and vary considerably in geometry. In this orientation spatial considerations will limit the extent to which cells can travel along any particular axis [9]; this is one reason why we find active migration to be untenable explanation for the extent to which cells penetrate our scaffolds over the first 24hr of culture. Any migration across the fiber axis and into the scaffold would

necessarily be highly tortuous and cover far more distance than the linear measured distance between adjacent tissue sections. There is no clear way to fabricate an electro spun matrix that more closely mimics the heterogeneity of fiber polarity that exists in vivo. It does not seem likely that scaffolds composed of fibers traveling in the X-Y axis and Z axis can co-exist in the same electro spun structure. We have attempted to provide a mechanical gradient by fabricating scaffolds composed of fibers that vary in diameter as a function of the Z direction in a scaffold [10]. These constructs are highly resistant to delamination failures, but do not appear to promote any more extensive cell penetration than conventional scaffolds. We believe the material properties of the individual fibers that make up the mechanical gradient are “out of range” for the cells to actually detect (fibers are too stiff).

We were successful in this study at promoting the infiltration of the scaffolds using a cyclic trypsin digest. This treatment would be expected to disrupt any cell-matrix interactions formed as a result of fibronectin, vitronectin, other serum constituents and or cellular activity. The loss of these adhesions will cause the cells to round-up and perhaps makes them more susceptible to sieving into the scaffolds. The impact of this treatment on increasing cell division also cannot be discounted as a mode by which the enzyme functions to increase cell number inside the scaffolds [17-21]. If this type of intervention proves effective for other cell types it may be possible to populate scaffolds with a broad spectrum of cell types relatively easily and quickly, including differentiated cells that are ordinarily relatively immobile, like muscle cells. Ultimately, diffusion barriers will limit the extent to which tissue engineered materials can be populated in vitro. However, in order to successfully produce engineered tissues and organs the limits of that barrier must be fully explored and defined. Developing strategies to bump up against this barrier are critical to the future success of the tissue engineering paradigm.

References

1. Rothwell SW, Sawyer E, Dorsey J, Flournoy WS, Settle T, et al. (2009) Wound healing and the immune response in swine treated with a hemostatic bandage composed of salmon thrombin and fibrinogen. *J Mater Sci Mater Med* 20(10): 2155-2166.
2. Boland ED, Wnek GE, Simpson DG, Pawlowsk KJ, Bowlin GL (2001) Tailoring tissue engineering scaffolds using electrostatic processing techniques: a study of poly (glycolic acid) electro spinning. *Journal of Macromolecular Science, Part A* 38(12): 1231-1243.
3. Lee KH, Kim HY, Khil MS, Ra YM, Lee DR (2003) Characterization of nano-structured poly (ϵ -caprolactone) nonwoven mats via electrospinning. *Polymer* 44: 1287-1294.
4. McManus MC, Sell SA, Bowen WC, Koo HP, Simpson DG, et al. (2008) Electrospun fibrinogen-polydioxanone composite matrix: potential for in situ urologic tissue engineering. *Journal of Engineered Fibers and Fabrics* 3(2): 12-21.
5. Telemeco TA, Ayres CE, Bowlin GL, Wnek GE, Boland ED (2005) Cohen N Simpson DG. Regulation of cellular infiltration into tissue engineering scaffolds composed of submicron diameter fibrils produced by electrospinning. *Acta Biomater* 1(4): 377-385.

6. Curtis A, Wilkinson C (1997) Topographical control of cells. *Biomaterials* 18(24): 1573-1583.
7. Ehrbar M, Sala A, Lienemann P, Mosiewicz K, Bittermann A, et al. (2011) Elucidating the role of matrix stiffness in 3D migration and remodeling. *Biophys J* 100(2): 284-293.
8. Petrie RJ, Gavara N, Chadwick RS, Yamada KM (2012) Non polarized signaling reveals two distinct modes of 3D cell migration. *J Cell Biol* 197(3): 439-455.
9. Wolf K, Lindert M, Krause M, Alexander S, Te Riet J, et al. (2013) Physical limits of cell migration: Control by ECM space and nuclear deformation and tuning by proteolysis and traction force. *J Cell Biol* 201(7): 1069-1084.
10. Grey CP, Newton ST, Bowlin GL, Haas TW, Simpson DG (2013) Gradient fiber electro spinning of layered scaffolds using controlled transitions in fiber diameter. *Biomaterials* 34 (21): 4993-5006.
11. McClure MJ, Wolfe PS, Simpson DG, Sell SA, Bowlin GL (2012) The use of air-flow impedance to control fiber deposition patterns during electro spinning. *Biomaterials* 33(3): 771-779.
12. Grey CP, Simpson DG (2015) Frontal Cryosectioning: An Improved Protocol for Sectioning Large Areas of Fibrous Scaffolds. *Journal of Nano materials* 501: 359696.
13. Ware MD, Wells A, Lauffen BDA (1998) Epidermal growth factor alters fibroblast migration speed and directional persistence reciprocally and in a matrix dependent manner. *J Cell Science* 111(Pt 16): 2423-2432.
14. Harunaga JS, Yamada KM (2011) Cell-matrix adhesions in 3D. *Matrix Biol* 30(7-8): 363-368.
15. Jha BS, Ayres CE, Bowman JR, Telemeco TA, Sell SA, et al. (2011) Electrospun collagen: a tissue engineering scaffold with unique functional properties in a wide variety of applications. *Journal of Nano materials* doi.org/10.1016/j.arabjc.2015.11.015.
16. Carney DH and Cunningham DD (1977) Initiation of check cell division by trypsin action at the cell surface. *Nature* 268(5621): 602-606.
17. Chow WN, Simpson DG, Bigbee JW, Colello RJ (2007) Evaluating neuronal and glial growth on electrospun polarized matrices: bridging the gap in percussive spinal cord injuries. *Neuron Glia Biol* 3(2): 119-126.
18. Colello RJ, Chow WN, Bigbee JW, Lin C, Dalton D, et al. (2016) The incorporation of growth factor and chondroitinase ABC into an electrospun scaffold to promote axon re growth following spinal cord injury. *J Tissue Eng Regen Med* 10(8): 656-658.
19. Ehrbar M, Sala A, Lienemann P, Mosiewicz K, Bittermann A, et al. (2011) Elucidating the role of matrix stiffness in 3D migration and remodeling. *Biophys J* 100(2): 284-293.
20. Jha BS, Colello RJ, Bowman JR, Sell SA, Lee KD, Bigbee JW, et al. (2011) Two pole air gap electrospinning: fabrication of highly aligned, three-dimensional scaffolds for nerve reconstruction. *Acta Biomater* 7(1): 203-215.
21. Michael C McManus, Scott A Sell, Whitney C Bowen, Harry P Koo, David G Simpson, et al. (2008) Electrospun Fibrinogen-Polydioxanone Composite Matrix: Potential for In Situ Urologic Tissue Engineering. *J Eng Fiber Fabr* 3(2): 12-21.



This work is licensed under Creative Commons Attribution 4.0 License
DOI: [10.19080/JOJMS.2017.01.555565](https://doi.org/10.19080/JOJMS.2017.01.555565)

Your next submission with Juniper Publishers will reach you the below assets

- Quality Editorial service
- Swift Peer Review
- Reprints availability
- E-prints Service
- Manuscript Podcast for convenient understanding
- Global attainment for your research
- Manuscript accessibility in different formats
(Pdf, E-pub, Full Text, Audio)
- Unceasing customer service

Track the below URL for one-step submission
<https://juniperpublishers.com/online-submission.php>